Characterization of cerium doped yttrium gadolinium aluminate garnet $(Y\text{-}Gd)_3Al_5O_{12}:Ce^{3+}$ phosphor thin films fabricated by pulsed laser deposition

A H Wako[1]*, F B Dejene[1], H C Swart[2]
[1]Department of Physics, University of the Free State, QwaQwa Campus, Private Bag X13, Phuthaditjhaba 9866, South Africa
[2]Department of Physics, University of the Free State, P O Box 339, Bloemfontein, ZA-9300, South Africa

E-mail: wakoah@qwa.ufs.ac.za

Abstract. Thin films of cerium doped yttrium gadolinium aluminate garnet $(Y\text{-}Gd)_3Al_5O_{12}:Ce^{3+}$ (YGAG:Ce) were grown on Si(100) substrates by a pulsed laser deposition (PLD) technique using a 266 nm Nd:YAG pulsed laser under varying deposition conditions, namely; substrate temperature, substrate – target distance, number of laser pulses and the working atmosphere during the film deposition process. The effect of annealing temperatures on the structure and luminescence properties of the as-deposited (YGAG:Ce) thin films were analysed. Photoluminescence (PL) data were collected in air at room temperature using an F-7000 FL Spectrophotometer. A slight shift in the wavelength of the PL spectra was observed from the thin films when compared to the PL spectra of the phosphor in powder form, which is probably due to a change in the crystal field. The PL intensity of the samples increased as the annealing temperature was increased from 400 ^oC to around 700 ^oC and then decreased with continued increase in the annealing temperature.

1. Introduction

Yttrium aluminium garnet (YAG) has proved to be an excellent host material compatible with lanthanides and most trivalent rare earth dopants. YAG are mostly applied in solid state lasers especially the white light emitting diodes (LEDs) by incorporating them with suitable rare earth dopants. YAG activated by trivalent Cerium (Ce^{3+}) has excellent chemical and thermal stability and is also well known for good scintillators [1]. The optical band gap energy for YAG bulk powder is in the order of 6.6 eV comprising of filled O_2 2p orbitals in the valence band and empty 4d orbitals [2].
Yttrium-gadolinium aluminium gallium garnet $(Y\text{-}Gd)_3Al_5O_{12}:Ce^{3+}$ is a modified form of $Y_3Al_5O_{12}:Ce^{3+}$ where Ce^{3+} and Gd^{3+} are incorporated into the $Y_3Al_5O_{12}$ lattice such that Gd^{3+} substitutes Y^{3+} in the system $(Y_x\text{-}Gd_{1-x})_3Al_5O_{12}:Ce^{3+}$. Since the ionic radius of Gd^{3+} is larger than that of Y^{3+} replacing Y^{3+} with Gd^{3+} results in lattice expansion. This way depending on the concentration of Gd^{3+} the host matrix structure can be modified in order to blue-shift or red-shift the emission from the Ce^{3+}. $(Y\text{-}Gd)_3Al_5O_{12}:Ce^{3+}$ can efficiently absorb a wide range of excitation wavelengths from ultra-violet (UV) to visible light and it can give out a broad band emission in the spectral range of 510 nm to over 600 nm [3] which makes it suitable for white LED applications.

This colour shift can be attributed to the fact that the characteristic broad yellow emission band from the $5d^1$ - $4f^1$ transitions of Ce^{3+} is highly sensitive to changes in the chemical environment of the host which induces crystal-field effect in the lowest $5d^1$ orbital [4].

Several methods have been used to grow thin films such as Physical Vapour Deposition (PVD) and/or Chemical Vapour Deposition (CVD) [5], Chemical Bath Deposition [6], rf magnetron sputtering[7] pulsed laser deposition (PLD) [8] and epoxide-catalyzed sol-gel methods [9]. However PLD has several advantages over other techniques such as the homogeneous stoichiometric evaporation of the ablated material on to the substrate [5] and good quality thin films can be obtained at low temperatures [10] by varying parameters such as substrate distance, atmosphere and substrate temperature among others. These parameters affect the thickness, roughness and overall quality of the obtained films which in turn influence the structure and photoluminescence (PL) properties of $(Y\text{-}Gd)_3Al_5O_{12}:Ce^{3+}$ phosphor.
In this study thin films of $(Y\text{-}Gd)_3Al_5O_{12}:Ce^{3+}$ were prepared using PLD. The effect of different annealing temperatures on the structure and photoluminescent (PL) properties of the $(Y\text{-}Gd)_3Al_5O_{12}:Ce^{3+}$ thin films were investigated.

2. Experimental

A Commercial yellow $(Y\text{-}Gd)_3Al_5O_{12}:Ce^{3+}$ powder obtained from Phosphor Technology (UK) was pressed into a pellet and used as a target for laser deposition after initial characterization. The pellet was then heated at 200 °C for 2hrs in a furnace to expel moisture that may be present and make it hard and strong for use as a target for laser ablation. The target was then loaded on to a rotatable carousel inside a PLD chamber. The carousel raster and rotates the target to prevent constant ablation by the laser beam from the same spot on the target.
Silicon (100) wafers of approximately 1 cm^2 were used as substrates. The wafers were first cleaned in an ultrasonic bath of acetone, ethanol and distilled water in that sequence then blow-dried with clean dry N_2 gas and placed on a fixed substrate holder in the PLD chamber perpendicular to the target at a fixed distance of 4.5 cm form the target. The chamber was then pumped down to vacuum of about $3.0x10^{-6}$ mbar. The target was ablated using a 266 nm Nd:YAG nanosecond (ns) pulsed laser with energy and frequency fixed at 45mJ/pulse (fluence of 0.2 Jcm^{-2}) and 10Hz respectively.
The ablation of the $(Y\text{-}Gd)_3Al_5O_{12}:Ce^{3+}$ target was carried out in the PLD chamber with a vacuum pressure of 10^{-6} mbar at constant substrate temperature of 200 °C. To investigate the effect of annealing, the as-deposited films were first characterized and then post-annealed in air for 60 minutes at 400 °C, 800 °C and 1000 °C in an XD-1200 NT tube furnace. The room temperature PL excitation and emission fluorescence spectra were recorded using an F-7000 FL Spectrophotometer at scan speed of 60 nm/min at 400 PMT voltage and excitation and emission monochromator slit widths of 5 nm.
X-Ray Diffraction (XRD) continuous scans were recorded using a Bruker-AXS D8 Advance X-ray diffractometer operating at 40 kV and 4 mA using Cu Ka = 1.5406 nm from 15° to 65° (2θ), with a scan rate of 0.39° (2θ)/min and step scans with a step size of $0.02^0(2\theta)$.

3. Results and discussions

3.1. Structure

XRD patterns of the $(Y\text{-}Gd)_3Al_5O_{12}:Ce^{3+}$ phosphor powder and thin films that were post-calcined at 400 °C, 800 °C and 1000 °C are shown in figure 1(a). Except for impurity peaks the rest fitted well with the powder and the JCPDS card number 072-1315 for the cubic $Y_3Al_5O_{12}$ of space group Ia-3d(230), cell ratios a/b=1.0000 b/c=1.0000 c/a=1.0000 and cell parameters a=12.0160Å. FWHM is an indication of peak broadening [11]. From figure 1(a) it was observed that XRD peak broadening occurred with an increase in the annealing temperature up to around 700 ^oC (estimated from the smoothed curve) and then narrowed down as the temperature was increased to 1000 ^oC. This is also

displayed on figure 2(a) which shows the comparison of FWHM with annealing temperature. The average crystallite sizes calculated for the (420) direction were obtained using Scherrer's equation $D = K\lambda/(\beta \cos\theta)$ where D is the mean particle size, K is a geometric factor, λ is the X-ray wavelength and β is Full With at Half Maximum (FWHM).

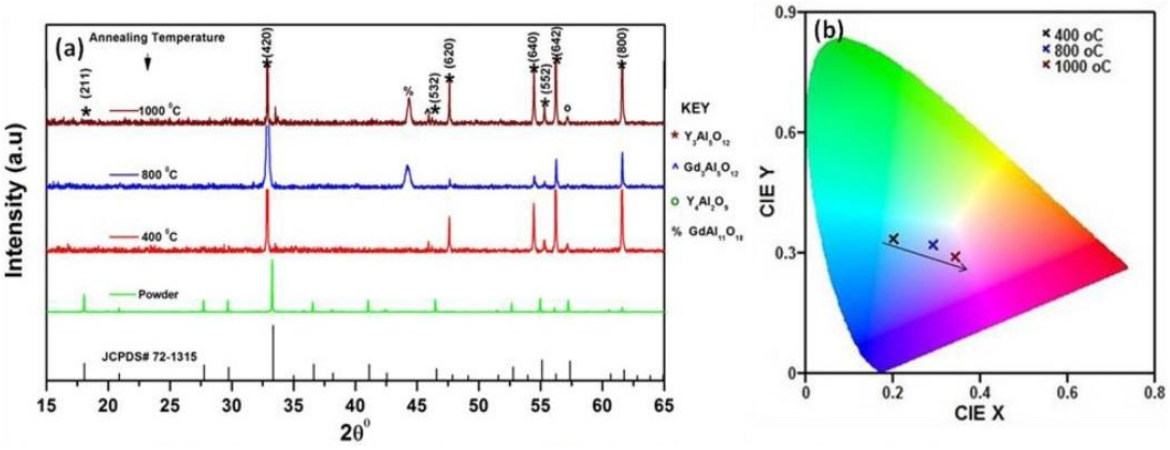

Figure 1. (a) XRD patterns of the $(Y\text{-}Gd)_3Al_5O_{12}:Ce^{3+}$ phosphor powder and thin films that were deposited in vacuum at 300 °C for 10 minutes and annealed at 400 °C, 800 °C and 1000 °C respectively and (b): CIE colour chromaticity as a function of annealing temperature.

Figure 2 (a) and (b) also shows how the crystallite size varied with annealing temperature. The crystallite size reduced as the temperature increased up to around 700 ^{o}C suggesting improved crystallinity and growth [11] but as annealing temperature increased above 700 ^{0}C, the sample was gradually losing crystallinity which could be attributed to phase change that may have introduced impurities. As was also reported by Y Deng et al that $Y_3Al_5O_{12}$: Gd thin films deposited at 700 ^{o}C were amorphous, supports this fact [7].

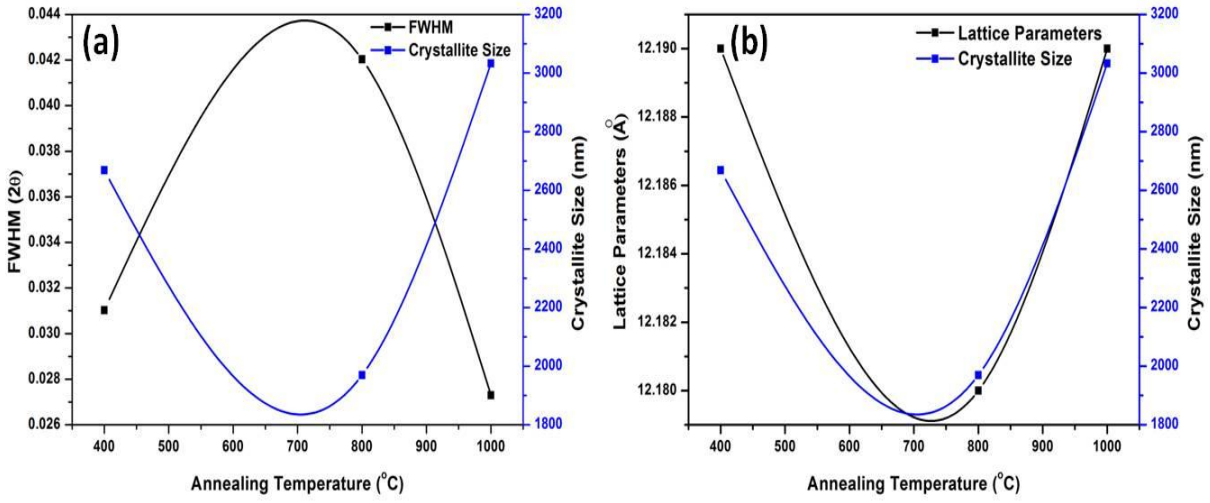

Figure 2(a) and (b). FWHM, Crystallite size and Lattice parameter as a function of annealing temperature.

It was also reported elsewhere that the phases;$Y_3Al_5O_{12}$ (cubic) and $YAlO_3$ (perovskite) were stable between room temperature and their melting points of 1970 and 1870 ^{o}C respectively but $Y_4Al_2O_9$ was

unstable below 1000 ^{o}C [12]. Yousif et al showed that new phases were formed after annealing the $Y_3(Al,Ga)_5O_{12}:Tb^{3+}$ films at temperatures greater than 1073 K[8].
From figure 2(b) we observed that the lattice parameters are also influenced by the annealing temperature in a similar manner. It was observed to decrease with increasing temperature up to around 700 ^{0}C.
It was also observed that diffraction peaks in the directions; (420), (552), (640) and (642) shift toward smaller angles compared to those of the $(Y\text{-}Gd)_3Al_5O_{12}:Ce^{3+}$ commercial powder and the JCPDS card #072-1315 which could be due to the impurities phases; $Gd_3Al_5O_{12}$,$Y_4Al_2O_9$ and $GdAl_{11}O_{18}$ that are formed as temperature was increased. It has been reported that the phases YAM ($Y_4Al_2O_9$), YAP ($YAlO_3$) and YAG ($Y_3Al_5O_{12}$) are often present in the Y_2O_3-Al_2O_3 system even if YAG is prepared stoichiometrically [13]. Therefore, this shift could be due to lattice expansion caused by differences in ionic radius when Y(r =0.104 nm) is substituted by Gd (r = 0.108nm) from the impurities phases [14] formed during the ablation process.
The crystallization temperature of the samples prepared by solid-state reaction (>1600 ^{0}C) is quite higher than the highest annealing temperature of 1000 ^{0}C in our experiment. But, during laser ablation, the temperature within the irradiated target volume rises rapidly exceeding the melting/boiling points of the target composition leading to explosive boiling because the laser heating rate significantly exceeds that of thermal diffusion and radiative losses [15].

3.2. Photoluminescence
Figures 3(a) and (b) show the PL excitation and emission spectra recorded from the $(Y\text{-}Gd)_3Al_5O_{12}:Ce^{3+}$ as-prepared powder and thin films annealed at 400 ^{0}C, 800 ^{0}C and 1000 ^{0}C. The PL emission spectra from the powder sample with a maximum at 546 nm is a broad band ranging from 450 nm to 650 nm when excited with 337 nm UV due to the 4f-5d electronic transition of Ce^{3+} attributed to the de-localization of electrons from the lowest 5d level to the crystal field split 4f ($^{2}F_{5/2}$ / $^{2}F_{7/2}$) levels of Ce^{3+}.

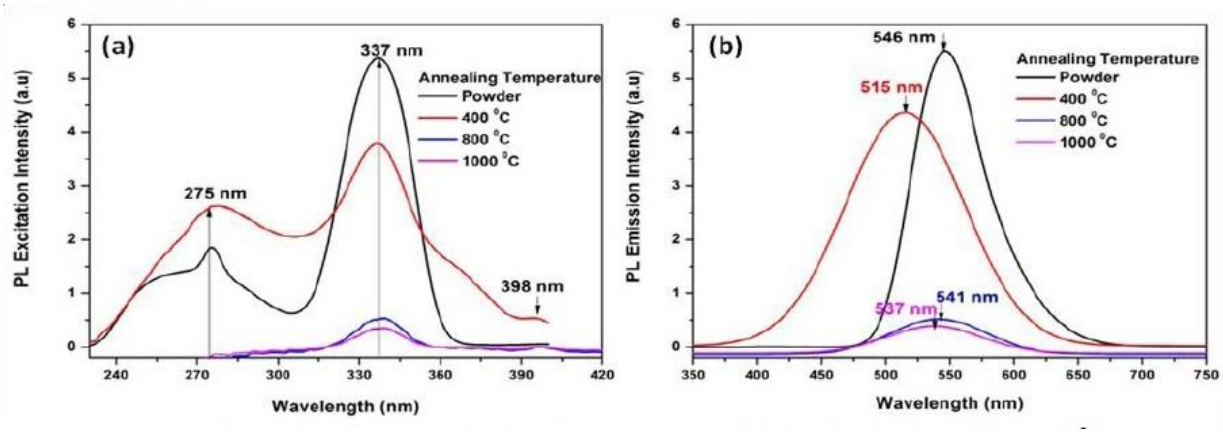

Figure 3 (a) and (b). Excitation and emission spectra of the $(Y\text{-}Gd)_3$ $Al_5O_{12}:Ce^{3+}$ phosphor powder and thin films that were deposited in vacuum at 200 ^{0}C for 10 minutes and annealed at 400 ^{0}C, 800 ^{0}C and 1000 ^{0}C respectively.

The normalized PL spectra for the annealed samples reveal changes in the peak positions and intensities relative to that of the powder sample. The PL intensity of the samples increased as the annealing temperature was increased from 400 ^{o}C to around 700 ^{o}C and then decreased with continued increase in the annealing temperature as shown in figure 4(a). Such observation was reported by Yousif et al who observed that intensity ratio of I_{490nm}/I_{544nm} and I_{625nm}/I_{544nm} for $Y_3(Al,Ga)_5O_{12}:Tb^{3+}$ phosphor, gradually decreased when the annealing temperature was increased from 1073 K (800 ^{o}C) to 1473 K (1200 ^{o}C) [8]. This can be attributed to stress and cracking that led to the diffusion of Si into

the film at higher temperatures [16]. Also it can be due to the impurity phases, $Gd_3Al_5O_{12}$ and $GdAl_{11}O_{18}$ that are higher in Gd concentration since it is well known that for a phosphor to exhibit the required properties, purity is very important. The PL intensities of the films are generally low in all cases compared to those of the powder of the same chemical composition due to total internal reflection in thin films [17]. However thin films have advantages over the powders in that they posses better thermal stability, better adhesion to the substrate, higher lateral resolution and less out gassing in device applications [8,18]. As shown in figure 3(b) the centers of the emission bands red-shift from 515 to 541 nm as the annealing temperature increased. This red-shift can be explained by an increase in the crystal field effect when the Y^{3+} vacancies are occupied by the larger Gd^{3+}. Since the ionic size of Gd^{3+} is larger than that of Y^{3+} it results in lattice expansion confirmed by the shifting of XRD peaks towards the smaller angles, which correlates with the red-shift of Ce^{3+} emission. The variation of the lowest crystal-field energy level of the $5d^1$ state is strongly influenced by the electrostatic field in the surrounding host lattice which in turn depends on the crystalline structure of the host $(Y\text{-}Gd)_3Al_5O_{12}$ lattice [3].

The CIE chromaticity co-ordinates of PL spectra of all the samples compared with the powder are shown in figure 1(b). It is clear that as the annealing temperature increases the co-ordinates shift to red as pointed out by the arrow. This is also supported by the PL spectra wavelength shifts in figure 3(b).

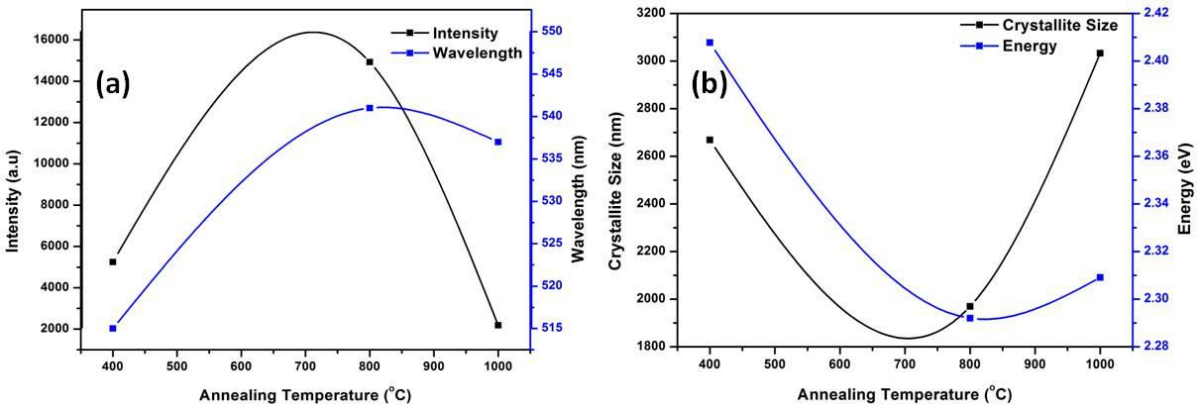

Figure 4: (a) PL intensity (a.u), Peak wavelength (nm) and **(b)** Peak Wavelength and band gap energy as a function of annealing temperature.

Figure 4(a) also shows how the PL wavelength peak positions vary as a function of annealing temperature. The wavelength peaks slightly shifted to higher wavelengths (red-shift) from 515 to 541 nm as the annealing temperature was increased from 400 – 800 ^oC and then blue-shifts to lower wavelengths at temperatures above 800 ^oC. The optical band gap calculated with respect to the PL peak positions shifted to a lower energy from 2.41 - 2.29 eV with increasing annealing temperature from 400 - 800 ^oC and then to higher energy 2.29 - 2.31 eV above 800 ^oC as shown in figure 4(b) . These changes have been attributed to the morphological dependent properties of the energy band gap [19]. 515 to 541 nm.The band gap of the thin film nanophosphors was calculated to be ~2.34 eV, which is generally red shifted in comparison to the band gap (~6.6 eV) of its bulk counterpart. The blue shift in band gap is a clear signature of nanostructure formationand may be attributed to the quantum size effect [20]

4. Conclusion

In this study thin films of $(Y\text{-}Gd)_3Al_5O_{12}:Ce^{3+}$ were prepared using the PLD technique. The effect of varied annealing temperature on the structure and PL properties of the $(Y\text{-}Gd)_3Al_5O_{12}:Ce^{3+}$ thin films were investigated. It was found that as the annealing temperature increase broadening of the XRD peaks occurs. Since the ionic size of Gd^{3+} is larger than that of Y^{3+} substitution of Y^{3+} with Gd^{3+} leads

to lattice expansion confirmed by the shifting of the XRD peaks towards the lower angles which in turn cause slight shifts in the wavelength of the PL spectra toward red with respect to the annealing temperature which is probably due to a change in the crystal field caused by lattice expansion.

Acknowledgments
In this study thin films of $(Y\text{-}Gd)_3Al_5O_{12}:Ce^{3+}$ were prepared using the PLD technique. The effect of varied annealing temperature on the structure and PL properties of the $(Y\text{-}Gd)_3Al_5O_{12}:Ce^{3+}$ thin films were investigated. It was found that as the annealing temperature increase broadening of the XRD peaks occurs. Since the ionic size of Gd^{3+} is larger than that of Y^{3+} substitution of Y^{3+} with Gd^{3+} leads to lattice expansion confirmed by the shifting of the XRD peaks towards the lower angles which in turn cause slight shifts in the wavelength of the PL spectra toward red with respect to the annealing temperature which is probably due to a change in the crystal field caused by lattice expansion.

References

[1] Potdevin A, Chadeyron G, Briois V and Mahiou R 2011 *Mater. Chem. Phys.* **130** 500
[2] Dlamini S T S, Swart H C, Terblans J J and Ntwaeaborwa O M 2013 *Solid State Sci*. **23** 6
[3] Pan Y X, Wang W, Liu G K, Skanthakumar S, Rosenberg R, Guo X Z and Li K K 2009 *J. Alloys Compd.* **488** 638
[4] Yousif A, Swart H C and Ntwaeaborwa O M 2013 *J. Lumin.* **143** 201
[5] Hirata G A, Lopez O A, Shea L E, Yi J Y, Cheeks T and Mckittrick J 1996 *J. Vac. Sci. Technol*. **14** 1694
[6] Koao L F, Dejene F B and Swart H C 2014 *Mater. Sci. Semicond. Process*. **27** 33
[7] Deng Y, Fowlkes J D, Rack P D and Fitz-Gerald J.M 2006 *Opt. Mater. (Amst)*. **29** 183
[8] Yousif A, Swart H C, Ntwaeaborwa O M and Coetsee E 2013 *Appl. Surf. Sci.* **270** 331
[9] Murai S, Verschuuren M A, Lozano G, Pirruccio G, Koenderink A F and Rivas J G 2012 *Opt. Soc. Am*. **2** 1707
[10] Sun X W and Kwok H S 1999 *Appl. Phys*. A **69** S39
[11] Chun-jia L I U, Rui-min Y U, Zhi-wei X U, Jing C A I, Xing-huang Y A N, Xue-tao L U O, Science M and Engineering C 2007 *Trans. Nonferrous Met. Soc. China* **17** 1093
[12] Cockayne, B. 1985 *J. Less-Comm.Met.***114** 199
[13] Huh Y, Cho Y and Do Y R 2002 *Bull. Korean Chem. Soc* **23** 1435
[14] Uysal S S, Ege A, Ayvacikli M, Khatab A, Ekdal E, Popovici E J, Henini M and Can N 2012 *Opt. Mater. (Amst)*. **34** 1921
[15] Ashfold M N R, Claeyssens F, Fuge G M and Henley S J 2004 *Chem. Soc. Rev*. **33** 23
[16] Yousif A, Swart H C and Ntwaeaborwa O M 2013 *Proc. Int. Conf. of South Africa Institute of Physics (Zululand)* p 1
[17] Choe J 2002 *Mater. Res Innov*. **6** 238
[18] Hillie K T, Ntweaeborwa O M and Swart H C 2004 *Phys. Status Solidi* **1** 2360
[19] Ezema F I, Ekwealor B C and Osuji R U 2006 *Turk J Phys* **30** 157
[20] Ankush V, Sanjeev G, Ravi K, Amit K C, Ramesh C, Nafa S, Keun H C 2012 *J. Alloys Compd.* **527** 1